Axon initial segment Ca^{2+} channels influence action potential generation and timing
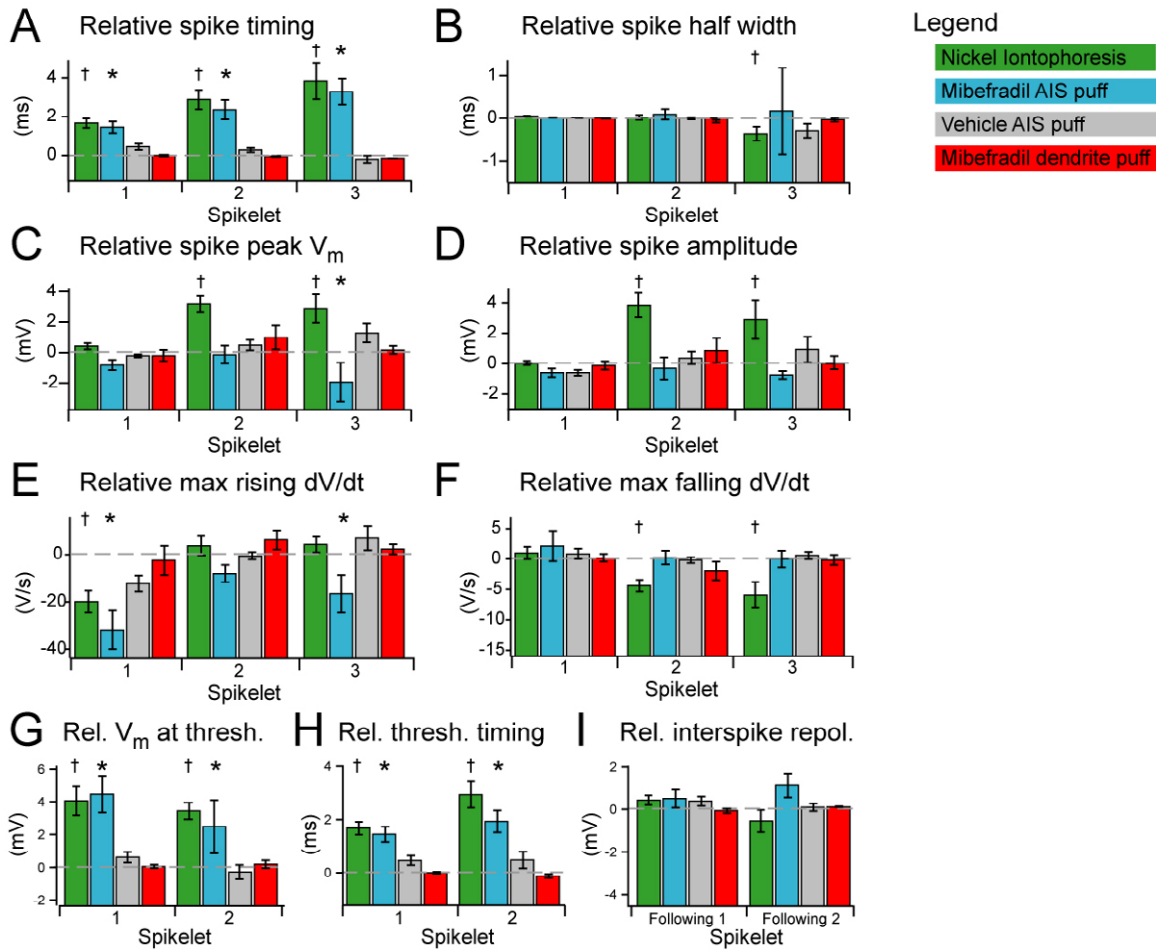
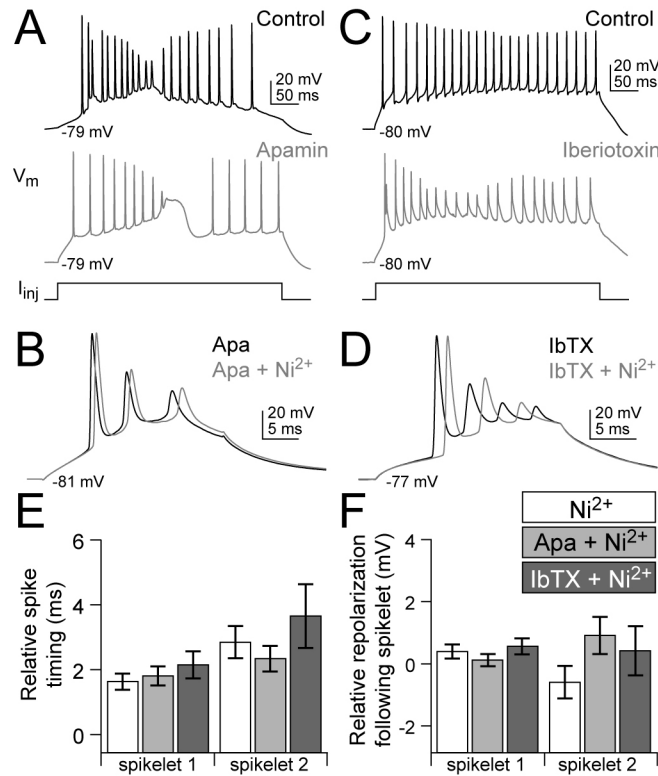Kevin J. Bender and Laurence O. Trussell

Supplemental Figure 1.

Complex spike parameters across mibefradil puff and Ni^{2+} iontophoretic experiments. All values are shown relative to control conditions. Green: Ni^{2+}; cyan: AIS mibefradil; grey: AIS vehicle; red: dendrite mibefradil. †: $p < 0.05$, Ni^{2+} vs. hypothetical mean, one sample t-test. *: $p < 0.05$, AIS mibefradil vs. AIS vehicle, Fisher's PLSD. Bars are SEM.

(A) Spike timing, measured at spike peak.
(B) Spike half width, measured half way from threshold V$_m$ to peak V$_m$.
(C) Peak spike voltage.
(D) Spike amplitude, measured from threshold V$_m$ to peak V$_m$.
(E) Maximum rising spikelet dV/dt.
(F) Maximum falling spikelet dV/dt.
(G) V$_m$ at threshold.
(H) Time of spike threshold.
(I) Peak interspike repolarization potential.
Data in panels (A) and (G) are the same as in Figs. 6 and 7.

Supplemental Figure 2.

Ca^{2+}-activated K$^+$ channels do not interact with AIS voltage-gated Ca^{2+} channels.
(A)   Cartwheel cell spike response to somatic current injection in control conditions (top), and with bath application of apamin (bottom). Note broadening of underlying complex spike depolarization.
(B)   Complex spikes paired with local AIS Ni^{2+} iontophoresis, as in Fig. 7, but in the presence of bath applied apamin (Apa).
(C)   Same as (A), but for iberiotoxin (IbTX). Note increased simple spike width and reduction in afterhyperpolarization.
(D)   Same as (B), but for IbTX. Note decrease in inter-spike repolarization magnitude.
(E)   Relative timing of spike peak for control (white), apamin (light grey) and IbTX conditions (dark grey). BK/SK-block conditions were not statistically different than Ni^{2+} iontophoresis alone.
(F)   Relative peak interspike repolarization potential. Conditions were not statistically different. Bars are SEM.